Progress In Electromagnetics Research B, Vol. 3, 255–269, 2008

FREQUENCY DOMAIN INTERFERENCE CANCELLATION FOR SINGLE CARRIER CYCLIC PREFIX CDMA SYSTEMS

F. S. Al-Kamali, M. I. Dessouky, B. M. Sallam and F. E. A. El-Samie

Department of Electronics and Electrical Communications
Faculty of Electronic Engineering
Menoufia University
Menouf, Egypt

Abstract—In this paper, we propose a low complexity receiver structure for Single-input Multiple-output (SIMO) downlink cyclic prefix CDMA (CP-CDMA) systems. It employs an interference cancellation scheme to suppress the interference caused by the multipath fading channel. Also, the proposed scheme is developed for Multiple-input Multiple-output (MIMO) CP-CDMA system. All filters in the proposed receiver are implemented in the frequency domain. The performance of the proposed receiver is studied and compared. Our results show a large performance improvement when using such an interference cancellation scheme relative to the rake receiver, and frequency domain Equalization (FDE).

1. INTRODUCTION

Broadband mobile communication systems are required to support high quality multimedia transmissions. However, there exist challenges including frequency selective channels, which are introduce by the multipath effect. Among the various alternatives proposed in the literature, many are based on CDMA due to its flexibility and low-cost of implementation. In addition to the effects of the Rayleigh channel, the performance of CDMA systems is mainly limited by interference from other users, which is called the multiple access interference (MAI). Recently, frequency domain equalization (FDE) has been shown to be an attractive solution for frequency selective channels in single carrier systems [1–3]. There are two approaches in CDMA technique: single carrier CDMA and multicarrier CDMA

(MC-CDMA). A lot of attention is paid to MC-CDMA. However, recently it has been shown that single carrier CDMA can achieve good performance comparable to MC-CDMA and orthogonal frequency division multiplexing (OFDM) if FDE is used. Furthermore, the single carrier CDMA was shown to have two main advantages over OFDM, namely, lower peak-to-average ratio and reduced sensitivity to carrier frequency error [2]. SIMO architecture is one of the most solutions for high data rate due to there enormous potential for capacity gains relative to single input single output (SISO) architecture. Also the use of MIMO for wireless communications produces significant performance improvements, including the reduction of bit error rates and the increase of capacity [4–6, 9]. However, channel equalization in broadband MIMO systems can potentially be very complex due to the superposition of all of the transmitted streams at each receive antenna. The complexity of the equalization process can be mitigated somewhat by performing equalization in the frequency-domain at the receiver [3, 6, 7]. In this paper, we propose a low Complexity frequency domain interference cancellation architecture for downlink SIMO and MIMO CP-CDMA systems. The proposed scheme uses the frequency domain parallel interference cancellation (FD-PIC) to subtract the interference in frequency domain before FDE. The efficiency of this scheme comes from the frequency domain implementation of all filters. The performance of this scheme is studied and compared.

The difference between FD-PIC in our proposed scheme and frequency domain interchip interference cancellation (FD-ICI) in Takeda & Adachi's scheme [7] is that in FD-ICI, the residual ICI is regenerated and subtracted in the frequency domain from each frequency component after FDE. But, in FD-PIC, another type of interference (MAI) is regenerated in frequency domain and subtracted before FDE.

The rest of this paper is organized as follows. We start in Section 2 by describing frequency domain interference cancellation for downlink SIMO CP-CDMA system. In Section 3, frequency domain interference cancellation for downlink MIMO CP-CDMA system is discussed. Simulation results and concluding remarks are presented in Sections 4 and 5, respectively.

Notations: Throughout the paper, $(.)^{\mathbf{H}}$, $(.)^{\mathbf{T}}$, and $(.)^{-1}$ are used to denote complex conjugate transpose of a matrix, transpose of a matrix, and inverse of a matrix, respectively. Vectors and matrices are represented in boldface. Ψ^{-1} and Ψ are used to represent the fast Fourier transform (FFT) matrix and the inverse fast Fourier transform (IFFT) matrix, respectively.

2. SIMO CP-CDMA SYSTEM

2.1. System Model

We consider the downlink transmission in a single cell CDMA system with K users and N_r receiver antennas. At the transmitter, each user transmits BPSK information symbols. Those symbols are spread with spreading code. After spreading, the resulting signal is scrambled using complex scrambling sequence and a cyclic prefix of N_{CP} chips is added at the beginning of each block to form a the transmitted block. Downlink CP-CDMA transmitter and the transmitted block are shown in Fig. 1.

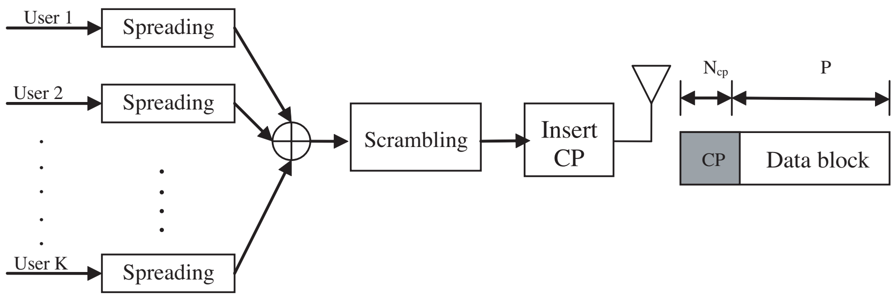

Figure 1. Downlink CP-CDMA transmitter and transmit block.

The propagation channel is assumed to be frequency selective fading channel having L discrete paths. The discrete-time impulse response $h_j(t)$ of multipath channel observed by the jth $(1 \leq j \leq N_r)$ receive antenna can be expressed as:

$$h_j(t) = \sum_{l=0}^{L-1} h_{j,l}\delta(t - \tau_l) \tag{1}$$

where $h_{j,l}$ is the l-th path complex gain experienced at the jth antenna. The chip sequence received on the jth antenna can be expressed as [7]:

$$r_j(t) = \sum_{l=0}^{L-1} h_{j,l}d(t - \tau_l) + n_j(t) \tag{2}$$

where n_j is the noise, and $d(t)$ is the transmitted signal. In matrix notation, the received signal is represented as:

$$\mathbf{r} = \mathbf{H}_{\mathrm{CT}}\mathbf{d} + \mathbf{n} = \mathbf{H}_{\mathrm{CT}}\mathbf{d}_{\mathrm{des}} + \mathbf{H}_{\mathrm{CT}}\mathbf{d}_{\mathrm{int}} + \mathbf{n} \tag{3}$$

The notations are listed below:

$$\mathbf{r} = [\mathbf{r_1} \ \ldots \ \mathbf{r_{Nr}}]^{\mathbf{T}} \tag{4}$$

$$\mathbf{H_{CT}} = [\mathbf{H_{C1}} \ \ldots \ \mathbf{H_{CNr}}]^{\mathbf{T}} \tag{5}$$

$$\mathbf{n} = [\mathbf{n_1} \ \ldots \ \mathbf{n_{Nr}}]^{\mathbf{T}} \tag{6}$$

where:

$\mathbf{H}_{\mathrm{C}j}$: is a circulant Toeplitz matrix of the jth channel.

$\mathbf{d}$: is the data vector.

$\mathbf{n}_j$: is the noise vector.

$\mathbf{d}_{\mathrm{des}}$: is a vector of the desired bits.

$\mathbf{d}_{\mathrm{int}}$: is a vector of the interference bits.

The vector $\mathbf{d}$ can be represented as:

$$\mathbf{d} = \mathbf{CSb} \tag{7}$$

where $\mathbf{C}$ is a scrambling code matrix, $\mathbf{S}$ is a block diagonal matrix whose diagonal consists of the spreading codes, and $\mathbf{b}$ is a vector consisting of the users' amplitudes and the transmitted bits. After removal the cyclic prefix from the received signal, the received signals are transformed into frequency domain, and the FFT of the received signal is given by:

$$\mathbf{R} = \Lambda\mathbf{D} + \mathbf{N} = \underbrace{\Lambda\mathbf{D}_{\mathrm{des}}}_{\textbf{useful diversity}} + \underbrace{\Lambda\mathbf{D}_{\mathrm{int}}}_{\textbf{MAI}} + \underbrace{\mathbf{N}}_{\textbf{Noise}} \tag{8}$$

where:

$$\mathbf{D}_{\mathrm{des}} = \Psi^{-1}(\mathbf{CS_d b}_{\mathrm{des}}) = \Psi^{-1}(\mathbf{d}_{\mathrm{des}}) \tag{9}$$

$$\mathbf{D}_{\mathrm{int}} = \Psi^{-1}(\mathbf{CUb}_{\mathrm{int}}) = \Psi^{-1}(\mathbf{d}_{\mathrm{int}}) \tag{10}$$

$$\mathbf{N} = [\mathbf{N_1} \ \ldots \ \mathbf{N_{Nr}}]^{\mathbf{T}} \tag{11}$$

$$\Lambda = [\Lambda_{\mathbf{1}} \ \ldots \ \Lambda_{\mathbf{Nr}}]^{\mathbf{T}} \tag{12}$$

$$\mathbf{R} = [\mathbf{R_1} \ \ldots \ \mathbf{R_{Nr}}]^{\mathbf{T}} \tag{13}$$

where $\mathbf{S_d}$ is the spreading code of the desired user, $\mathbf{U}$ is a matrix containing the spreading codes of the interfering users, $\mathbf{b}_{\mathrm{des}}$ is the desired user data, $\mathbf{b}_{\mathrm{int}}$ is a vector containing the interfering users' data, and Λ_j is a diagonal matrix containing the FFT of the circulant sequence of $\mathbf{H}_{\mathrm{C}j}$.

The first term of Eq. (8) represents the useful diversity, the second term is MAI, and the third term is due to noise.

2.2. Frequency Domain Interference Cancellation for Downlink SIMO CP-CDMA Systems

Figure 2 is the block diagram (two-antenna example) of the proposed receiver for SIMO downlink CP-CDMA systems. It uses SIMO FDE to estimate the interfering bits. Then, FD-PIC is used to regenerate, and cancel the MAI in the frequency domain. After that, the SIMO FDE is used to provide a better estimate of desired user's data. The proposed scheme is called SIMO FDE-PIC scheme.

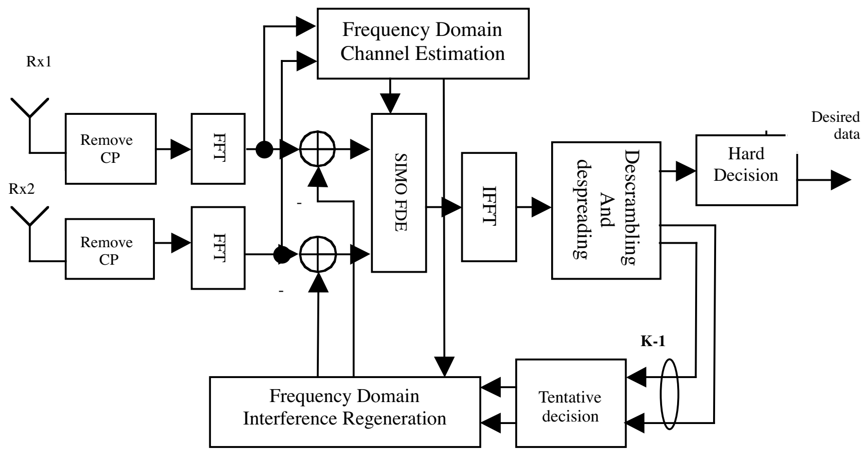

Figure 2. The proposed SIMO FDE-PIC scheme when $Nr = 2$.

Based on the received frequency domain signal in Eq. (8), the SIMO FDE can be employed as follows:

$$\hat{\mathbf{D}} = \mathbf{WR} \tag{14}$$

where:

$$\mathbf{W} = [\mathbf{W_1},\ \ldots,\ \mathbf{W_{Nr}}] \tag{15}$$

$\mathbf{W}_j$ can be chosen according to the channel parameter Λ_j and minimum mean square error (MMSE) criterion:

$$\mathbf{W}_j = \Lambda_j^{\mathbf{H}} \left(\Lambda_j \Lambda_j^{\mathbf{H}} + \left(\frac{\sigma_j^2}{\sigma_{\mathbf{d}}^2} \right) \mathbf{I_0} \right)^{-1} \tag{16}$$

where σ_j^2 is the variance of the additive noise at the jth antenna, and $\sigma_{\mathbf{d}}^2$ is the variance of the transmitted signal. Then, the equalized frequency domain signal is converted to the time domain with an IFFT operation as follows:

$$\hat{\mathbf{d}} = \Psi(\hat{\mathbf{D}}) \tag{17}$$

The transmitted data symbols of the interfering users are obtained after descrambling and despreading. The estimates of the symbols obtained here are the first decision made, and we refer to this as tentative decision. This step can be written as:

$$\hat{\mathbf{b}}_{\text{int}} = \mathbf{f}_{\text{dec}}(\mathbf{U}^{\mathbf{T}}\mathbf{C}^{\mathbf{H}}\hat{\mathbf{d}}) \tag{18}$$

Where f_{dec} is a tentative decision. The tentative decision data is then spread and scrambled using the corresponding codes and a replica of the interfering signal is reconstructed with the channel parameters and FFT operation. The interfering signal can be written as:

$$\mathbf{R}_{\mathbf{MAI}} = \Lambda\hat{\mathbf{D}}_{\text{int}} \tag{19}$$

where:

$$\hat{\mathbf{D}}_{\text{int}} = \Psi^{-1}(\mathbf{CU}\hat{\mathbf{b}}_{\text{int}}) \tag{20}$$

The interfering signal is subtracted from the original received signal as follows.

$$\mathbf{Z} = \mathbf{R} - \mathbf{R}_{\mathbf{MAI}} \tag{21}$$

After interference cancellation, SIMO FDE is performed as follows:

$$\mathbf{D}_{\text{Final}} = \mathbf{WZ} \tag{22}$$

Finally, the desired user's symbols can be obtained after IFFT operation, descrambling and despreading as follows:

$$\hat{\mathbf{b}}_{\text{des}} = \mathbf{sign}\left(\mathbf{real}\left(\mathbf{S}_{\mathbf{d}}^{\mathbf{T}}\mathbf{C}^{\mathbf{H}}\Psi\left(\hat{\mathbf{D}}_{\text{Final}}\right)\right)\right) \tag{23}$$

We refer to this decision as the final decision. In order to improve the performance further, the suggested algorithm can be implemented in multistage. However, multistage implementation leads to increase the complexity.

The main advantage of this receiver are that, in addition to provide greater performance and capacity when compared to the FDE-PIC in SISO scenario, all filters in the receiver are implemented in the frequency domain. However, its complexity increases if the number of receiving antennas increased.

2.3. Complexity Analysis and Practical Issue

- **Complexity**
  We evaluate the computation complexity by counting only the number of complex multiplications in computation of equalizer weights and the received signals processing for each block as in [6]. The complexity of our proposed scheme is shown in Table 1, compared to the complexity of the conventional SIMO FDE, and SISO FDE-PIC. It can be observed that SIMO FDE-PIC has reasonable complexity as compared to SIMO FDE, and SISO FDE-PIC. This suggests that the proposed structure is more suitable for high data rate systems that requiring good BER performance.

Table 1. Complexity of the proposed SIMO FDE-PIC scheme compared to SIMO FDE, and SISO FDE-PIC.

Tasks	SIMO FDE	SISO FDE-PIC	SIMO FDE-PIC
Equalization Weight	$Nr^3P/3 + 2Nr^2P$	$2P/3 + 4P$	$2Nr^3P/3 + 4Nr^2P$
FFT	$NrP(\log_2 P)/2$	$P(\log_2 P)/2$ $+P(\log_2 P)/2$	$NrP(\log_2 P)/2$ $+P(\log_2 P)/2$
IFFT	$P(\log_2 P)/2$	$P(\log_2 P)$	$P(\log_2 P)$
Equalization	NrP	$2P$	$2NrP$
Regenerated in Frequency domain	0	P	NrP

- **Practical issue**
  Its possible to reduce the complexity of the proposed structure by skipping the FD-PIC stage if not necessary. This may be the case when the system is weakly loaded.

3. MIMO CP-CDMA SYSTEM

MIMO transmission techniques are divided into two classes: space-time coding (STC) and spatial multiplexing. So far most researchers in MIMO CDMA focus on the STC CDMA system [8]. This paper proposes a MIMO CDMA system that employing Vertical Bell labs LAyered Space Time architecture (V-BLAST).

3.1. System Model

The structure of a MIMO CDMA transmitter that employing V-BLAST with K users can be depicted as in Fig. 3. In this system, three types of interference should be suppressed at the mobile station: (1) multiple access interference (MAI) (2) interantenna interference (IAI); (IAI exists between different base station's antennas) (3) Inter-symbol interference (ISI) due to the multipath distortion. As shown in Fig. 3, each user's data are demultiplexed to Nt substreams by the V-BLAST demultiplexer. Then the substreams of one user are spread by the same signature sequence. After spreading, the resulting signal is scrambled using complex scrambling sequence and a cyclic prefix of N_{CP} chips is added at the beginning of each block to form a transmit block. The result substreams are transmitted through Nt antennas.

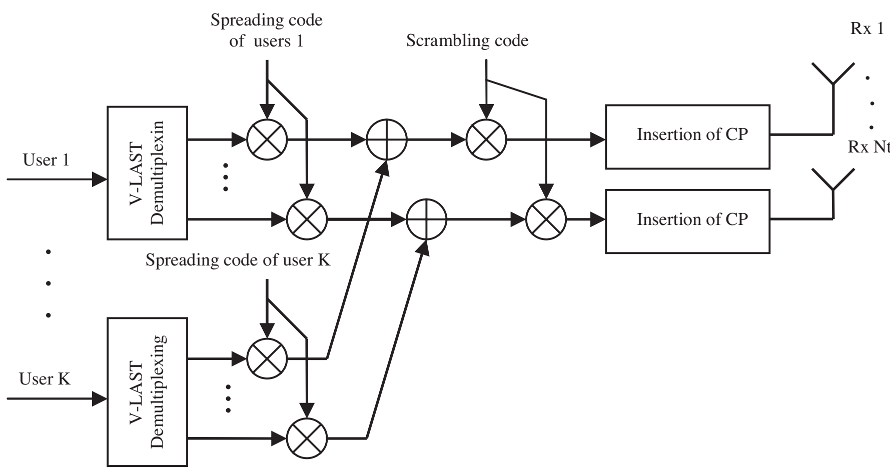

Figure 3. Single-carrier cyclic prefix assisted MIMO downlink CDMA system.

In order to prevent inter-cell interference scrambling code is applied to the transmission data streams. At the receiver, the cyclic prefix is discarded to prevent the interblock interference. The mth ($m = 0, \ldots, \mathrm{M} - 1$) sample of the received signal at the jth receiver antenna ($1 \leq j \leq Nr$) elements can be expressed as [6]:

$$r_j[m] = \sum_{i=1}^{Nt} \sum_{l=0}^{L-1} d_i(m-l) h_{j,i}[l] + z_j(m) \tag{24}$$

where $d_i(m)$ are the chips transmitted by the ith antenna, $h_{j,i}(l)$ is the channel impulse response coefficient between the ith transmit antenna and the jth receive antenna.

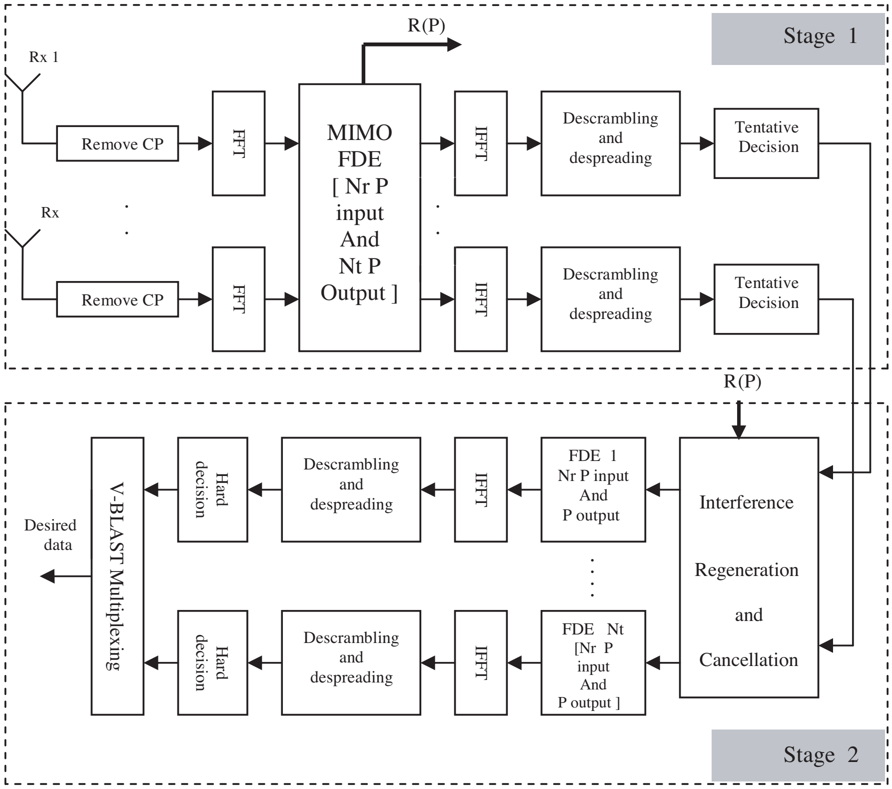

Figure 4. The structure of the suggested MIMO FDE-PIC for downlink MIMO CP-CDMA systems.

3.2. Frequency Domain Interference Cancellation for Downlink MIMO CP-CDMA Systems

This section describes the suggested frequency domain interference cancellation for downlink MIMO CDMA systems. The suggested scheme is called MIMO FDE-PIC and it is shown in Fig. 4. It consists of two stages. At the first stage, the cyclic prefix is discarded to prevent the interblock interference (IBI). Then, the received signals are transformed into frequency domain, and the pth frequency tone of the received signal can be written as:

$$\mathbf{R}(p) = \mathbf{H}(p)\mathbf{D}(p) + \mathbf{N}(p) \tag{25}$$

where:

$$\mathbf{R}(p) = [R_1(p),\, R_2(p),\, \ldots\,,\, R_{Nr}(p)]^{\mathbf{T}} \tag{26}$$

$$\mathbf{D}(p) = [D_1(p),\, D_2(p),\, \ldots\,,\, D_{Nt}(p)]^{\mathbf{T}} \tag{27}$$

$$\mathbf{N}(p) = [N_1(p),\, N_2(p),\, \ldots\,,\, R_{Nr}(p)]^{\mathbf{T}} \tag{28}$$

And

$$\mathbf{H}(p) = \begin{bmatrix} \mathrm{H}_{1,1}(p) & \mathrm{H}_{1,2}(p) & \cdots & \mathrm{H}_{1,Nt}(p) \\ \mathrm{H}_{2,1}(p) & \mathrm{H}_{2,2}(p) & \cdots & \mathrm{H}_{2,Nt}(p) \\ \cdots & \cdots & \cdots & \cdots \\ \mathrm{H}_{Nr,1}(p) & \mathrm{H}_{Nr,2}(p) & \cdots & \mathrm{H}_{Nr,Nt}(p) \end{bmatrix} \tag{29}$$

$R_j(p)$: is the pth frequency tone at the jth receive antenna. $\mathbf{H}(p)$ can be simply expressed as:

$$\mathbf{H}(p) = [\mathbf{H}_1(p)\ \mathbf{H}_2(p)\ \ldots\ \mathbf{H}_{Nt}(p)] \tag{30}$$

After that, a series of MIMO-FDE, IFFT, descrambling, despreading and tentative decision is carried out to obtain the tentative decisions. The output of the MIMO FDE can be written as:

$$\hat{\mathbf{D}}(p) = \mathbf{W}(p)\mathbf{R}(p) \tag{31}$$

where [6]:

$$\mathbf{W}(p) = \mathbf{H}^{\mathbf{H}}p\left(\mathbf{H}(p)\mathbf{H}^{\mathbf{H}}(p) + N_o\mathbf{I}\right)^{-1} \tag{32}$$

At the second stage of the MIMO FDE-PIC, the tentative decisions of the interferers from the first stage are cancelled from the received signal in frequency domain. The regenerated interference signals in frequency domain from the i-th transmit antenna can be written as:

$$\mathbf{V}^{(i)}(p) = \mathbf{H}_i(p)\hat{\mathbf{D}}_i(p) \tag{33}$$

The modified received signal associated to the n-th transmit antenna is given by:

$$\mathbf{Z}^{(n)}(p) = \mathbf{R}(p) - \sum_{i=1,\, i\neq n}^{Nt} \mathbf{V}^{i}(p) \tag{34}$$

The MMSE based FDE weight with the ith transmit antenna is then:

$$\mathbf{W}_i(p) = \mathbf{H}_i^{\mathbf{H}}(p)\left(\mathbf{H}_i(p)\mathbf{H}_i^{\mathbf{H}}(p) + N_o\mathbf{I}\right)^{-1} \tag{35}$$

Finally, the desired user's data can be obtained after IFFT operation, descrambling, despreading, hard decision, and VBLAST multiplexing.

4. SIMULATION RESULTS

Simulations have been carried out in two different ways: BER of the desired user versus the SNR, and BER of the desired user versus the number of active users. The channel is assumed to be frequency-selective Rayleigh fading channel having chip-spaced 3-path uniform power delay profile (i.e., $E[|h_l|^2] = 1/L$ for all l). More details of the simulation parameters are given in Table 2. All users are assigned the same power.

Table 2. Simulation parameters.

Modulation	BPSK, QPSK
Spreading codes	OVSF codes with processing gain 16
Scrambling codes	Complex scrambling sequence
Multipath channel	$L = 3$-path, uniform power delay profile
FFT points	$P = 256$
Cyclic prefix	$N_{\mathrm{CP}} = 16$
Equalization	LMMSE equalizer

Case1: SIMO: In this case, The performance of the proposed SIMO FDE-PIC is compared to that of SIMO FDE, SISO FDE-PIC, and the RAKE receiver. In this case, each user transmits BPSK information symbols.

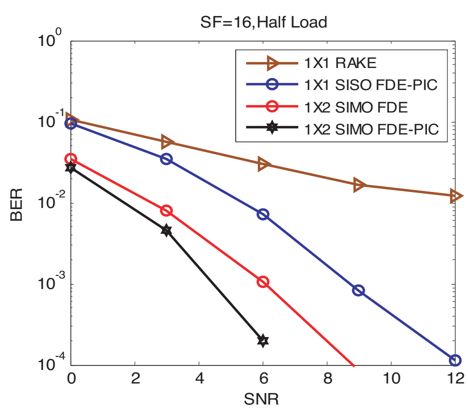

Figure 5. Performance of different reception schemes Vs the SNR for K = 8 (half load).

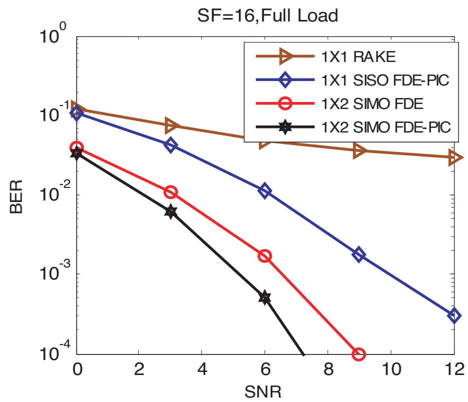

Figure 6. Performance of different reception schemes Vs the SNR for K = 16 (Full load).

Figures 5 and 6 show the BER as a function of the SNR for K = 8 (half load), and K = 16 (full load), respectively. As shown in Figs. 5 and 6, the proposed SIMO FDE-PIC scheme is effective in reducing the ISI and the MAI. It improves the performance significantly, especially at high SNR. With the proposed scheme, an SNR reduction of about 2 dB is achieved for BER $= 10^{-4}$ from the SIMO FDE (Fig. 6). For a full loaded case, with a typical BER level of 10^{-3}, the required SNR for SISO FDE- PIC detector has to be no less than 10 dB, whereas the required SNR for SIMO FDE-PIC is about 5 dB, which demonstrates a 5 dB improvement.

In Fig. 7, we represent the BER for different number of users. It obvious from the figure that the BER of the SIMO FDE-PIC is much lower than the BER of RAKE receiver, SISO FDE-PIC, and SIMO FDE. From the results, we can see that SIMO FDE-PIC increases the number of users of the system about 4 times than that of the SIMO FDE receiver.

To show the impact of the channel estimation on the performance of the SIMO FDE-PIC, and SIMO FDE, Fig. 8 illustrates the performance in terms of the BER versus the SNR. We use the LMMSE frequency domain channel estimation, where a training sequence is used. The degradation in SNR from ideal channel estimation for achieving BER $= 10^{-3}$ is 3 dB.

Figure 8 shows that the performance of the proposed scheme depends heavily on the channel estimation accuracy. This is because SIMO FDE-PIC uses the channel coefficients not only for the detection step, but also for the interference regeneration step.

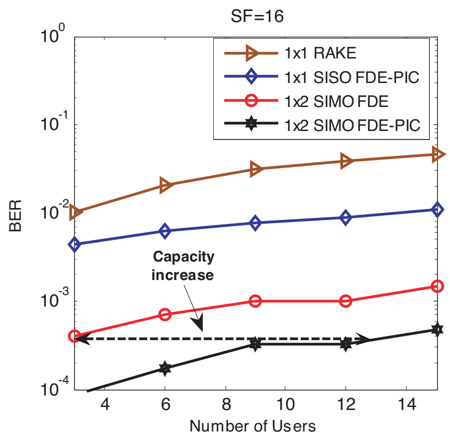

Figure 7. Performance of different reception schemes Vs the number of active users. SNR = 6 dB.

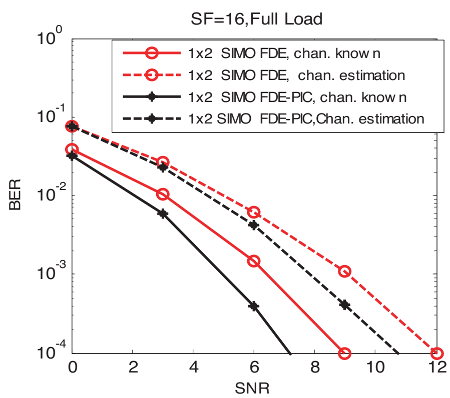

Figure 8. Performance of SIMO FDE-PIC, and SIMO FDE Vs the SNR for exact and LMMSE channel estimate.

Case 2 MIMO: In this case, we compare the performance of MIMO FDE-PIC, and MIMO FDE under synchronous MIMO channels. Simulation environment is based on the downlink synchronous MIMO CP-CDMA system in which each user transmits QPSK information symbols. Perfect channel estimation, $Nt = 2$, and $Nr = 2$ are assumed. The Rayleigh frequency selective fading channel is considered.

Figure 9 depicts the BER performance as a function of SNR. Here K = 16, and SF = 16. The figure shows that the MIMO FDE-PIC receiver achieves a remarkable gain compared to the MIMO

FDE receiver. With a BER level of 10^{-4}, the required SNR for the MIMO FDE receiver has to be 20 dB, whereas the required SNR for the suggested MIMO FDE-PIC is 16 dB, which demonstrates a 4 dB improvement.

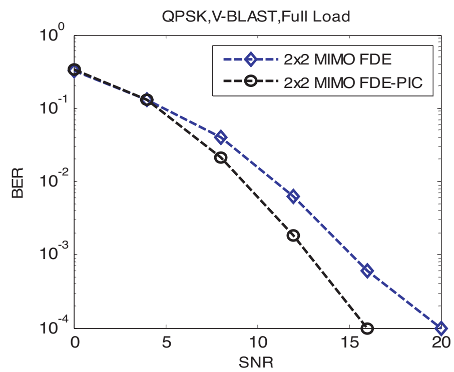

Figure 9. Performance of different reception schemes Vs the SNR for K = 16 (full load).

Figure 10 shows the BER versus the number of users in the system with SNR = 10 dB, and SF = 16. The performance curves show that the MIMO FDE-PIC improves the error performance significantly compared to the MIMO FDE.

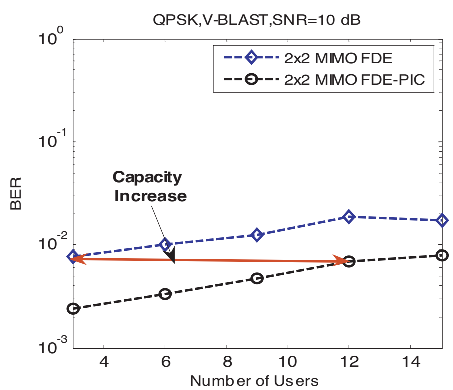

Figure 10. Performance of different reception schemes Vs the number of active users. SNR = 10 dB.

From the results, we can see that the MIMO FDE-PIC receiver increases the number of users of the system bout 4 times than that of the MIMO FDE receiver.

5. CONCLUSION

In this paper, we have proposed efficient receiver structure for downlink SIMO and MIMO CP-CDMA transmissions. The efficiency of the proposed structure is obtained by implementing all filters in the frequency domain through efficient FFT. The comparison studies show that the proposed receiver offers a large performance improvement with reasonable complexity relative to the rake receiver, SIMO FDE, and SISO FDE-PIC. The obtained results indicate that the performance of the proposed scheme is more efficient when the system load is high and a reliable communication is possible with the proposed scheme.

REFERENCES

1. Falconer, D., et al., "Frequency domain equalization for single-carrier broadband wireless systems," *IEEE Common. Mag.*, Vol. 40, 58–66, April 2002.
2. Adachi, F., D. Garge, S. Takaoka, and K. Takeda, "Broadband CDMA techniques," *IEEE Wireless Communications*, Vol. 12, No. 2, 8–18, April 2005.
3. Martoyo, I., T. Wesis, F. Capar, and F. Jondral, "Low complexity CDMA downlink receiver based on frequency domain equalization," *Proc. IEEE Vech. Tech. Conf.*, 987–991, Oct. 2003.
4. Foschini, G. J., "Layered space-time architecture for wireless communication in a fading environment when using multi-element antennas," *Bell Labs Technical Journal*, 1996.
5. Abouda, A. A. and S. G. Häggman, "Effect of coupling on capacity of MIMO wireless channels in high SNR scenario," *Progress In Electromagnetic Research*, PIER 65, 27–40, 2006.
6. Zhu, X. and R. D. Murch, "Novel frequency-domain equalization architectures for a singlecarrier wireless MIMO system," *IEEE VTC*, Vol. 2, 874–878, Vancouver, Canada, Sept. 2002.
7. Takeda, K., K. Ishihara, and F. Adachi, "Downlink DS-CDMA transmission with joint MMSE equalization and ICI cancellation," *IEEE Veh. Technol. Conf.*, Vol. 4, 1762–1766, Spring, 2006.
8. Alamouti, S. M., "A simple transmit diversity technique for wireless communications," *IEEE Journal Selected Areas on Communications*, Vol. 16, 1451–1458, Oct. 1998.
9. Geyi, W., "Multi-antenna information theory," *Progress In Electromagnetics Research*, PIER 75, 11–50, 2007.